Eur. Phys. J. B (2010)
DOI: 10.1140/epjb/e2010-00064-y

THE EUROPEAN PHYSICAL JOURNAL B

Regular Article

Higher-order phase transitions on financial markets

A. Kasprzak[1,a], R. Kutner[1], J. Perelló[2], and J. Masoliver[2]

[1] Faculty of Physics, University of Warsaw, Smyczkowa Str. 5/7, 02678 Warsaw, Poland
[2] Departament de Física Fonamental, Universitat de Barcelona, Diagonal, 647, 08028 Barcelona, Spain

Received 5 July 2009 / Received in final form 2 January 2010
Published online 23 February 2010 –

Abstract. Statistical and thermodynamic properties of the *anomalous* multifractal structure of random interevent (or intertransaction) times were thoroughly studied by using the extended continuous-time random walk (CTRW) formalism of Montroll, Weiss, Scher, and Lax. Although this formalism is quite general (and can be applied to any interhuman communication with nontrivial priority), we consider it in the context of a financial market where heterogeneous agent activities can occur within a wide spectrum of time scales. As the main general consequence, we found (by additionally using the Saddle-Point Approximation) the scaling or power-dependent form of the partition function, $Z(q')$. It diverges for any negative scaling powers q' (which justifies the name *anomalous*) while for positive ones it shows the scaling with the general exponent $\tau(q')$. This exponent is the nonanalytic (singular) or noninteger power of q', which is one of the pilar of higher-order phase transitions. In definition of the partition function we used the pausing-time distribution (PTD) as the central one, which takes the form of convolution (or superstatistics used, e.g. for describing turbulence as well as the financial market). Its integral kernel is given by the stretched exponential distribution (often used in disordered systems). This kernel extends both the exponential distribution assumed in the original version of the CTRW formalism (for description of the transient photocurrent measured in amorphous glassy material) as well as the Gaussian one sometimes used in this context (e.g. for diffusion of hydrogen in amorphous metals or for aging effects in glasses). Our most important finding is the third- and higher-order phase transitions, which can be roughly interpreted as transitions between the phase where high frequency trading is most visible and the phase defined by low frequency trading. The specific order of the phase transition directly depends upon the shape exponent α defining the stretched exponential integral kernel. On this basis a simple practical hint for investors was formulated.

1 Introduction

For the last few decades, the analysis of time-series has been an area of systematically increasing scientific activity [1–6][1]. Thanks to the progress in development of semi-analytical methods, including different detrending techniques developed by physicists [7–12] as well as to the progress in numerical recipes[2], the theory of time-series applies to an ever increasing amount of branches of knowledge. For example, the evolution of many complex systems in natural, economic, and social sciences is usually presented in the form of stochastic time series [13,14]. These series quite often represent multifractal stochastic processes [15] generated, e.g. by particularly useful noisy interscale multiplicative cascades (cf. [16] and references therein) observed, for instance, on speculative markets [17]. Moreover, variations of their indices, stock prices, returns and foreign exchange rates show an intermittent behaviour [18], manifest hierarchical and self-affine structures, and exhibit large (non-Gaussian) deviations [19] related to extreme events and fat tails of statistics. For a long time it has been well known (cf. [20] and references therein) that on financial markets the space variables, for example the most useful ones as indices, stock prices, returns, and exchange rates as well as time variables, such as interevent (or intertransaction) times and first-passage times, can be considered as stochastic variables and form stochastic time series. Indeed, the continuous-time random walk (CTRW) formalism and its different versions are ready to treat both space and time variables in a stochastic way providing a promising phenomenological description of tick-by-tick stochastic dynamics.

[a] e-mail: Andrzej.Kasprzak@fuw.edu.pl

[1] See also any volume of the *Journal of Time Series Analysis*, edited by M.B. Priestley.

[2] See, for example, *Mathematica. A system for Doing Mathematics by Computer, ver. 6.1* by S. Wolfram and *SAS for Forecasting Time Series, Second Edition*, by J. Brocklebank and D. Dickey.

The canonical CTRW formalism was originally introduced by Montroll and Weiss in 1965 [21] as a way to render time continuous. Since it had been first successfully applied by Scher and Lax in 1973 (cf. [21–28] and references therein) and independently by Moore one year later [29], to describe the anomalous transient photocurrent (manifesting the power-law relaxation) in amorphous glassy material, this formalism has achieved much more than its original goal, finding innumerable applications in many fields, and recently, e.g. in the field of financial markets ([1,30,31]). It provided there a dynamical description (in the stochastic sense) of the microstructure of random systems (see also [32–45]).

The pausing-time distribution (PTD), called also the waiting-time distribution (WTD), was defined within the CTRW formalism as a key sharp distribution. Originally, this distribution was defined within the so-called valley model. In this model energetic landscape consists only of valleys, i.e. no mountains are present. The basic, dynamic part of this PTD was the conditional WTD, $\psi(\Delta t|\varepsilon)$, being again the sharp probability distribution. It means that a given carrier stays exactly for a waiting-time interval Δt within the potential valley (before it makes a jump) under the condition that the depth of the valley is ε indeed. The conditional WTD (which in the context of the financial market is called the conditional pausing-time distribution while in our case it is the conditional distribution of intertransaction or interevent times) can be reinterpreted in the context of the financial market simply by reinterpretation of the stochastic variables Δt and ε. Recently, we gave [1] a list of other potential applications. In this work we were interested in the statistical properties of interevent times because they include the indispensable information concerning human communications in financial markets in particular. These properties are much less known than the corresponding statistical properties of "space" variables. In our recent paper [1] we extended the CTRW formalism to cover the multifractal structure of random intertransaction times. This structure is one of the most prominent features of the financial stochastic time series (cf. [46] and references therein). On this basis we are able to realize the main goal of the present work. It consists, in application of the thermodynamic formalism by using the Legendre transformation, for finding and discussing possible higher-order phase transitions, so rarely observed in the real world [47].

1.1 List of main enterprises

Previously [1] we derived averages of arbitrary order q (or q-moments) of the intertransaction times on financial markets, $\langle \Delta t^q \rangle$, within the extended CTRW formalism. We called it the multifractal continuous-time random walk (MF-CTRW) model. Our present work extends this approach, namely

- within the MF-CTRW formalism and also by using our refined heuristic formula, we consider pausing-time q-moments of intertransaction (interevent) times, $\langle \Delta t^q \rangle$, for a wider range $-1 < q \leq 20$ than that used formerly [1] since it includes also the negative values of q;
- only on this basis we consider the generalized partition function [48,49], $Z(q')$, expressed by the $q'(=q+1)$-moment of coarse-grained probability p (defined by the joint PTD), which is our main concern.

Owing to our earlier work [1], which proves that moments of interevent times satisfy the scaling relation (cf. also Eq. (19) in the present work), we demonstrate here that the partition function also takes a scaling form. This form results from the correspondence between crucial integrals, i.e. $I(q)$ (defined by Eq. (9)) and $J(q')$ (given by Eq. (32)),

$$J(q+1) = \sigma \frac{\exp(-q\lambda\mu)}{(q+1)^{1/\alpha}}\, I\left(-\frac{q}{(q+1)^{1/\alpha}}\right), \qquad (1)$$

where $q' = q+1 > 0$ or $q > -1$. In words, if integral $I(q)$ can be written in a scaling form then also $J(q')$ has the corresponding scaling form, and vice versa.

The analysis of $Z(q')$ provides formal correspondence between the MF-CTRW model and equilibrium thermodynamics. Here, we consider:

(i) the spectrum of singularities, which can be considered as an analogy of the entropy dependence on energy; and
(ii) 3rd- and higher-order phase transitions, which can be roughly interpreted as a transition between the phase of high and that of low frequency trading mostly visible.

The present paper is organized in the following manner. First (Sect. 2), we consider the scaling relation for q-moments $\langle \Delta t^q \rangle$ within the MF-CTRW formalism and compare them with corresponding empirical data. Hence, we found parameters needed for further analysis. Then (Sect. 3), we include scaling of the partition function, $Z(q')$, defined within the MF-CTRW formalism, its multifractal analysis, and derivation of the thermodynamic formalism for our case. Subsequently, Section 4 presents discussion of the 3rd- and higher-order phase transitions. Finally, Summary and concluding remarks are in Section 5 while some important technical details in Appendix A.

2 Pausing-time q-moments: multifractality generated by fluctuations

Roots of the model we propose herein are in physics. This model is also a reminiscence of the Mixture of Distribution Hypothesis[3] in finance, which can be traced back to the early 1970s [50,51] (and references therein), the variational principle of energy dissipation at the different time and spatial scales in turbulence being developed in the

[3] The Mixture of Distribution Hypothesis says that it is possible to consider a convolution of several distributions as a proper description of the complex financial system. In our case the convolution of two distributions sufficed.

1990s [52,53] (and references therein), as well as of superstatistics and nonextensive entropy [54] (and references therein). Moreover, it is a direct consequence of the multifractal version of our CTRW [1].

The main goal of this section is to calculate in a closed form, within the MF-CTRW formalism, the pausing-time moment of intertransaction times, $\langle \Delta t^q \rangle$ of arbitrary order $q > -1$. Hence, the basis is established (in Sect. 3) for developing thermodynamics (in Sect. 4) in terms of the partition function.

2.1 Superstatistics and q-moments

2.1.1 Exact calculations

As usual, we define the q-moment (for arbitrary real q) within the CTRW formalism, as follow

$$\langle \Delta t^q \rangle = \int_0^\infty \Delta t^q \psi(\Delta t) d\Delta t = \int_{-\infty}^\infty \langle \Delta t^q \mid \varepsilon \rangle \rho(\varepsilon) d\varepsilon, \quad (2)$$

where the pausing-time distribution, $\psi(\Delta t)$, is given[4] by the following superposition in the form of superstatistics [55,56],

$$\psi(\Delta t) = \int_{-\infty}^\infty \psi(\Delta t \mid \varepsilon) \rho(\varepsilon) d\varepsilon, \quad (3)$$

and conditional PTD is defined in the Poisson form

$$\psi(\Delta t \mid \varepsilon) = \frac{1}{\gamma(\varepsilon)} \exp\left(-\frac{\Delta t}{\gamma(\varepsilon)}\right). \quad (4)$$

This means that conditional intertransaction times are statistically independent, which can be assumed as a reasonable null hypothesis. Here, the conditional event (marked by parameter ε) means that the last transaction was realized indeed for the volume ε. In this context, the Poisson variable Δt is the intertransaction time counted from the moment of this last transaction to the moment of the next one while the mean intertransaction time for the volume ε (i.e., $\gamma(\varepsilon)$) is the arithmetic average over all these time intervals counted for fixed volume ε. We also assume it to be expressed in the exponential form

$$\gamma(\varepsilon) = \gamma_0 \exp(\lambda \varepsilon). \quad (5)$$

From empirical data we found that λ is, at most, slowly varying function of ε. However, its statistical error is too large to be meaningful. The most stable quantities appeared to be q-moments of intertransation times discussed below. Moreover, we can assume that ε is a positive number for the purchase of futures and negative for their sale where the purchase and sale are defined in the usual way[5].

The conditional pausing-time moment is easily calculated from expression (4):

$$\langle \Delta t^q \mid \varepsilon \rangle = \int_0^\infty \Delta t^q \psi(\Delta t \mid \varepsilon) d\Delta t = \Gamma(1+q)\, \gamma^q(\varepsilon). \quad (6)$$

Indeed $\Gamma(1+q)$, which appears in (6), confines our approach to $q > -1$. However, it is sufficient to permit the analysis of phase transition at $q = 0$.

Notably, it is difficult to measure both conditional quantity (4) and (6), as well as the mean time (5) given for fixed ε as they are burdened by large statistical errors. Moreover, the superstatistics (3) rather poorly depends on the detailed structure of $\gamma(\varepsilon)$ (cf. the plot of the sojourn probability vs. time [1], which at least partially supports this inference).

The next, crucial step of the approach is the proper selection of weight $\rho(\varepsilon)$ in the form of the stretched exponent, so often used in disordered systems:

$$\rho(\varepsilon) = \frac{1}{2^{1+1/\alpha}\, \sigma\, \Gamma(1+1/\alpha)} \exp\left(-\frac{1}{2}\left(\frac{\mid \varepsilon - \mu \mid}{\sigma}\right)^\alpha\right). \quad (7)$$

That way derivation (at least approximate) of equation (2) in a closed form is possible. In fact, this distribution appeared to be the crucial one. Hence, α was selected as the driving parameter for further investigations.

By combining expressions (6) and (7) with the second equation in (2) we get the (real, unconditional) q-moment $\langle \Delta t^q \rangle$ in the intermediate form ready for approximate analysis,

$$\langle \Delta t^q \rangle = \frac{\tau_0^q\, \Gamma(1+q)}{2^{1+1/\alpha} \sigma \Gamma(1+1/\alpha)}\, I(q), \quad (8)$$

where

$$I(q) \stackrel{\text{def.}}{=} \int_{-\infty}^\infty d\varepsilon \exp\left(-\frac{1}{2}\left(\frac{\mid \varepsilon - \mu \mid}{\sigma}\right)^\alpha + q\lambda\varepsilon\right). \quad (9)$$

As it is seen, both conditional (6) and unconditional (8) q-moments of interevent times are well defined only for $q > -1$ due to q-dependence of the $\Gamma(1+q)$ function.

2.1.2 Approximate calculations

The q-moment of the intertransaction (pausing) time intervals given by (8) was calculated in our work [1] by us-

[4] Indirectly, it was roughly verified in [1] by comparison the sojourn (decumulative) probability, $\Psi(t) = \int_t^\infty \psi(\Delta t) d(\Delta t)$, with empirical histogram of futures contracts, for example, on stocks of Telefonica.

[5] We deal with the purchase transaction of futures when the order to buy futures is indeed realized; it means that the corresponding order to sale futures had earlier been applied and was waiting until the purchase offer appeared. Definition of the sale transaction is analogous. Namely, we deal with the sale transaction of futures (having negative ε) when the order to buy futures had earlier been applied and waited until the sale offer appeared. If it happened that offers to buy and sale appeared at the same time the sign of ε is chosen at random.

ing the Saddle-Point Approximation[6] (SPA). For $\alpha > 1$ we obtained the following result:

$$\frac{\langle \Delta t^q \rangle}{\Gamma(1+q)} \approx \frac{\langle \Delta t^q \rangle_l}{\Gamma(1+q)} L^{|q|^{\alpha/(\alpha-1)}}, \tag{10}$$

where prefactor

$$\frac{\langle \Delta t^q \rangle_l}{\Gamma(1+q)} = \gamma_0^q l^q \tag{11}$$

scales with[7]

$$l \stackrel{\text{def.}}{=} \exp(\lambda\,\mu). \tag{12}$$

This means that this prefactor is related to dissipation since it depends on the $\lambda\mu(= \langle \lambda\varepsilon \rangle)$ shift[8], where $\langle \ldots \rangle$ means the average over the distribution $\rho(\lambda\varepsilon)$.

Besides, the scale

$$L \stackrel{\text{def.}}{=} \exp(b), \tag{13}$$

used in equation (10), is responsible for fluctuation since

$$b = \omega_0^{-1} \left(2^{1/\alpha} \lambda\sigma\right)^{\alpha/(\alpha-1)} \tag{14}$$

(where $\omega_0 = \alpha^{\alpha/(\alpha-1)}/(\alpha-1)$, cf. Eq. (67) in Appendix A) depends on

$$\lambda\sigma = \sqrt{\frac{\alpha}{2^{2/\alpha}} \frac{\Gamma(1+1/\alpha)}{\Gamma(3/2)}}\, \sigma_{\lambda\varepsilon}, \tag{15}$$

where variance $\sigma^2_{\lambda\varepsilon} = \langle (\lambda\varepsilon - \lambda\mu)^2 \rangle$ and $\langle \ldots \rangle$ means (as previously) the average over the distribution $\rho(\lambda\varepsilon)$. Moreover, by assuming the order $q = 1$ in equation (10), we obtain scale L in the form

$$L = \frac{\langle \Delta t \rangle}{\langle \Delta t \rangle_l}. \tag{16}$$

This form eliminates the monofractal pattern. It means that L is defined only by the fraction of the mean of the intertransaction times that is driven by fluctuations.

The q-moment $\langle \Delta t^q \rangle_l$ is the quantity characterizing monofractal. This is because it can be obtained by assuming that $\rho(\varepsilon) = \delta(\varepsilon - \mu)$, which is the result of the limit $\sigma \to 0$ in (7) (being an unrealistic case where volume fluctuations are absent). Relation (11) gives a plausible interpretation of scale l by assuming, again, $q = 1$, namely

$$l = \frac{\langle \Delta t \rangle_l}{\gamma_0}. \tag{17}$$

Hence, equation (11) becomes

$$\frac{\langle \Delta t^q \rangle_l}{\Gamma(1+q)} = \left(\langle \Delta t \rangle_l\right)^q. \tag{18}$$

By introducing equations (18) and (16) into (10), we obtain the general formula

$$\frac{\langle \Delta t^q \rangle}{\Gamma(1+q)} = \left(\langle \Delta t \rangle_l\right)^q \left(\frac{\langle \Delta t \rangle}{\langle \Delta t \rangle_l}\right)^{|q|^{\alpha/(\alpha-1)}} \tag{19}$$

where all quantities have well defined interpretations. We found that q-moments are expressed (in general) by singular, noninteger power of q and they scale with the ratio of two different first-order moments of the mean intertransation times. Equation (19) suggests that our PTD is such a broad distribution that a hierarchy of exponents is needed to characterize it. This feature results from the multifractal nature of our system. However, no signature evidence of any phase transition is found if one only searches for q-moments.

2.2 First results and refined heuristic formula

Previously [1] we discussed, for example, futures at six basic instruments. Three of them (DAX, WIG20, and the US Dollar-Deutsche Mark, USDM, exchange rate) have $3/2 < \alpha < 2$, two of them (TEF and DJI) have $\alpha \approx 3/2$ and one of them (the EURUS exchange rate) has $\alpha \approx 2$. Nevertheless, the logarithm of intertransaction time moments for futures at these basic financial instruments exhibits the analogous nonlinear q-dependence, although the number of data points changes from 282 007 for WIG20 to 4 997 027 for DAX. Hence, it seems to be reasonable to consider here transactions only for a chosen, most typical basic instrument.

Here, we decided to consider, for example, the future contracts at the USDM rate on Forex. The specification of these archival, empirical tick-by-tick intertransaction data used is as follows [1]. We chose quotation of these futures since 1993-01-04 until 1997-07-31, which consists of 1 048 590 data points.

In Table 1 we present:

(i) four values of the shape exponent α as well as combined parameters a ($\stackrel{\text{def.}}{=} \ln(\gamma_0) + \lambda\mu$) and b (the latter defined by Eq. (14)) obtained from the fit of the formula[9]

$$\ln\left(\frac{\langle \Delta t^q \rangle}{\Gamma(1+q)}\right) \approx a\,q + b \mid q \mid^{\alpha/(\alpha-1)} \tag{20}$$

to empirical data within, e.g., four increasing ranges of q; and

(ii) the corresponding values of the control parameter of the fit, χ^2/m (where m is the number of degrees of freedom) for these ranges of q.

[6] In the literature, the Saddle-Point Approximation is also called the Steepest-Descent Method or the Parabolic Extrapolation Method.

[7] All q-moments (given by Eqs. (10) and (11), as well as by the general and exact formulas (2), (6) and (8)) obey the normalization condition, i.e. they are equal to 1 for $q = 0$, as expected.

[8] Unfortunately, in our approach we are unable to find separately parameter λ.

[9] Formula (20) was derived from equation (10) where expressions (11), (12) and (13) were used.

Table 1. Fitted values of the MF-CTRW parameters α, a and b together with the control parameter χ^2/m obtained by the fit of formula (20) to empirical data within, for example, four different ranges of q.

Range of q	α	a	b	χ^2/m
0−3	1.754 ± 0.080	3.008 ± 0.011	0.2268 ± 0.0087	0.00012
0−4	2.04 ± 0.12	2.827 ± 0.039	0.394 ± 0.031	0.00049
0−5	2.48 ± 0.47	2.49 ± 0.20	0.710 ± 0.170	0.00131
0−6	3.18 ± 0.28	1.89 ± 0.15	1.27 ± 0.14	0.00261

In Table 1, we present results of fits for the range of $q \geq 3.0$ since only then the fits supply reliable values of the shape exponent α. This means that the difference between the empirical and straight curves is insufficient (cf. Fig. 2) to consider multifractality for shorter ranges of q. However, for a longer q range, the quantity χ^2/m is too large. Therefore, the exponent $\alpha = 1.754 \pm 0.080$ (and the corresponding values of the remaining parameters), obtained for the fit within the first q-interval, seems to be an optimal choice (used in our further considerations, cf. Tab. 2).

The upper solid curve in Figures 1 and 2 shows the prediction of formula (20). This prediction is obtained by fitting formula (20) to empirical data (marked by dots) within the shortest range of q, i.e. for $0 \leq q \leq 3$. In these figures we also marked two inflection points[10] of the empirical curve found for the particular orders $q = q^0_{ip} \approx 0$ and $q = q^1_{ip} \approx 6.48$ (cf. the intersection of the corresponding solid and dashed vertical straight lines with the empirical curve). These inflection points are very important since they split the whole range of q into three different regions. The first one, $-1 < q < q^0_{ip}$, the second one, $q^0_{ip} \leq q \leq q^1_{ip}$, and the third one, $q > q^1_{ip}$ where the q-moment is a concave, convex, and again concave function of q, respectively. Within the MF-CTRW formalism, we are able to systematically study (with a good approximation) first and second ranges of q. The systematic analysis of the third range still remains as a challenge, though, further in this section the heuristic formula is shown, which fits well the empirical curve for the whole range of q.

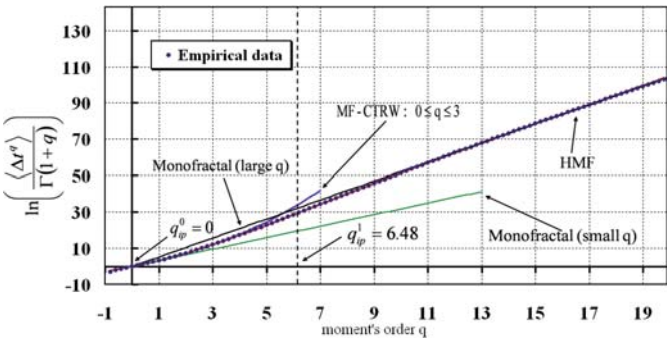

Fig. 1. (Color online) Semi-logarithmic plot comparing empirical data for q-moment $\langle \Delta t^q \rangle / \Gamma(1+q)$ vs. order q (concerning futures at USDM rate on Forex, marked by dots) with two different theoretical predictions given by formulas (20) (the upper curve, marked by MF-CTRW: $0 \leq q \leq 3$) and (21) (the lower one, which satisfactorily fits the empirical data in the whole range of q, marked by HMF), respectively. Moreover, the inflection points of the empirical curve for $q = q^0_{ip} \approx 0$ and $q = q^1_{ip} \approx 6.48$ are marked.

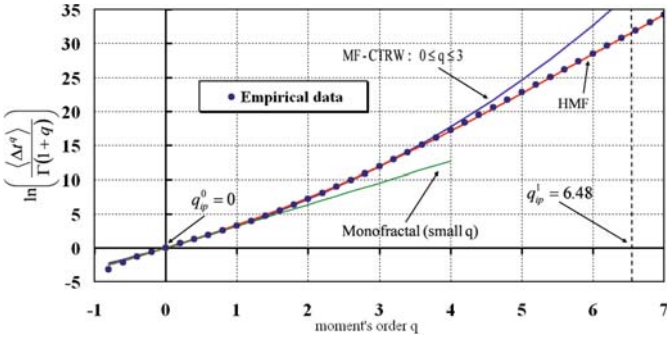

Fig. 2. (Color online) Magnification of the initial and central parts of Figure 1. The comparison of the empirical data (marked by dots) with the corresponding theoretical predictions. (i) The upper solid curve, given by formula (20), is extended to negative value of $q = -0.8$ and (ii) the lower limit, given by expression (21), is more distinct than that in Figure 1.

2.2.1 Guess of the refined heuristic formula

Formula (10) is the basis for the more advanced heuristic one, which must fit well the empirical data within the whole accessible range of q, here $-1 < q \leq 20$. This means that this formula for $\ln\left(\frac{\langle \Delta t^q \rangle}{\Gamma(1+q)}\right)$ must at least fulfill the following requirements:

(i) the normalization condition (i.e. for $q = 0$ the formula should be equal to 0);
(ii) for small, non-negative values of q the formula should become (with good approximation) the natural logarithm of formula (10), which is a convex function of q;
(iii) for the negative values of q (here within the range $-1 < q < 0$) the formula should be a concave function of q to fit well the empirical data (cf. Fig. 2);
(iv) for $q = q^0_{ip}$ the formula should provide the first inflection point, while for some intermediate q (here for $q = q^1_{ip} = 6.48$) it should provide the second one;
(v) for large values of q the formula should tend to the monofractal form.

Hence, such a formula can already be easily guessed

$$\frac{\langle \Delta t^q \rangle}{\Gamma(1+q)} \approx (\langle \Delta t \rangle_l)^q \, L_1^{\left[1 - L_2^{-|q|^{1/(\alpha-1)}}\right] q}, \qquad (21)$$

[10] The inflection point of a given function $\zeta(q)$ is defined by the equality $\frac{d^2\zeta(q)}{dq^2} = 0$ in this point and the requirement of the nonvanishing value of the second derivative in its vicinity.

Table 2. Set of the corresponding parameters of the MF-CTRW and the HMF formulas.

Model	α	a	b	b_1	b_2
MF-CTRW	1.754 ± 0.080	3.008 ± 0.011	0.227 ± 0.009	–	–
HMF	1.676 ± 0.018	3.074 ± 0.063	0.228 ± 0.028	2.152 ± 0.063	0.106 ± 0.010

where exponent b (given by expression (14)) is factorized

$$b = b_1\, b_2 \tag{22}$$

and the following definitions of scales are used

$$L_1 \stackrel{\text{def.}}{=} \exp(b_1),\ L_2 \stackrel{\text{def.}}{=} \exp(b_2). \tag{23}$$

The prediction of the HMF (Heuristic Multifractal) formula (21) was also shown in Figure 1 by the lower solid curve, which quite well fits the empirical data for the whole range of q. This prediction is additionally confirmed by magnifications shown in Figure 2 for the initial and intermediate values of q. As expected (see also Tab. 2) for the range $-0.5 \lesssim q \lesssim 3.5$ (essential for further considerations), the predictions of formulas (20) and (21) cannot practically be distinguished. In Table 2 we compare values of parameters defining both curves. Although these parameters are quite similar, in further considerations we use those predicted by formula (20) (the first row).

Moreover, predictions of the HMF formula (21) in Figures 1 and 2 are shown for the initial and asymptotic ranges of q converging to sloped straight lines[11]. These lines define the corresponding monofractals. Detailed results presented in these figures confirm that we have to deal with three different structures of interevent times. The main goal of the present work is to analyze the second, most important, multifractal structure of interevent times together with the one belonging to the left vicinity of $q = 0$.

It is possible to study our system by the partition function technique. This technique supplies cases of current interest in the investigation of multifractality of the structure of interevent times.

3 Partition function for the MF-CTRW formalism

In Section 2 above, we demonstrated that the q-moment of interevent times scales nonlinearly with the volume fluctuation. The important question arises if the partition function scales analogously as well. The aim of Sections 3 and 4 is to derive (at least approximately) the generalized partition function [48,49] in a closed form within the MF-CTRW model, and next, to consider

(i) important (complementary to those discussed in Sect. 2) multifractal properties of the structure of interevent times; and

(ii) its thermodynamic consequences, e.g. the possibility of higher-order phase transitions.

Initially, we use the following generalized form of the partition function [49], which is analogous to the grand partition function:

$$Z(q') = \frac{1}{\theta^{\,q'-1}} Z_0(q') = \left\langle \left(\frac{p_{\underline{i}}}{\theta}\right)^{q} \right\rangle,\ q' = q+1. \tag{24}$$

In the latter, the partition function

$$Z_0(q') = \sum_{\underline{i}} p_{\underline{i}}^{\,q'}, \tag{25}$$

and $\theta(>0)$ (defined self-consistently later on) relates to chemical potential for an open system, while two-component index $\underline{i} = (i_1, i_2)$ denotes a rectangle (with side length Δ_t[12] and Δ_ε, respectively). A coarse-grained probability (measure) $p_{\underline{i}}$ is attributed to this rectangle. By using such rectangles we can partition our phase space. In our approach (based on the MF-CTRW model), we consider the support of the measure, which is a two-dimensional, half-space continuum defined by the time interval $t \geq 0$ and the volume, ε, of traded futures that are bought or sold. Our measure vanishes only for $t \to \infty$ and/or $|\varepsilon| \to \infty$.

Both partition functions given by equation (24) obey (as it is required) the normalization condition, i.e.

$$Z(q' = 1) = Z_0(q' = 1) = 1. \tag{26}$$

It means that orders q' and q (used in the definition of q-moment (2)) are shifted by 1, i.e., $q' = q + 1$, which defines mutual calibration of both orders.

Moreover, one has

$$Z(q' \to 0) = Z_0(q' \to 0) \to \infty \tag{27}$$

since the substrate (defined by the Cartesian product of interevent time and futures volume) is unrestricted and all $p_{\underline{i}}$ values are nonvanishing (cf. expression (29)). This is the reason why (in our case) also $Z(q' < 0) = Z_0(q' < 0) = \infty$. Therefore, we have to restrict our considerations only to $q' > 0$.

For integer, nonvanishing q' values the partition function $Z_0(q')$ is the probability of finding q' transactions in any rectangle $\underline{i}$. In case of fixed q' values and different probabilities $p_{\underline{i}}$, the partition function $Z_0(q')$ increases for more heterogeneous values of $p_{\underline{i}}$. Therefore, for $q' \geq 2$ $Z_0(q')$ defines the chance of how close q' transactions are localized, i.e., it can measure the degree of heterogeneity

[11] Note that $\ln(\Delta t^q/\Gamma(1+q))$ tends linearly to zero from its both sides.

[12] Index t used here and in further considerations is equivalent to Δt used earlier.

of the structure or correlations between transactions. For example (as it follows from definition (25)), for full heterogeneity or localization at some rectangle $\underline{j}$ (then one has $p_{\underline{i}} = \delta_{\underline{i},\underline{j}}$), the partition function assumes its maximal value, $Z_0(q') = 1$. Moreover, for fixed $p_{\underline{i}} < 1$ and varying power q', the partition function decreases with increasing power. That is, correlations between transactions or the localization decrease when the number of transactions increases, as expected.

Next, we relate probabilities $p_{\underline{i}}$ to joint and conditional waiting-time distributions defined within our MF-CTRW formalism. Then, we define the generalized partition function, $Z(q')$, and perform calculations

$$\begin{aligned} Z(q') &\stackrel{\text{def.}}{=} \frac{1}{\theta^{\,q'-1}} \\ &\times \sum_{i_1=0}^{\infty} \sum_{i_2=-\infty}^{\infty} \left[\int_{t_{i_1}}^{t_{i_1}+\Delta_t} dt \int_{\varepsilon_{i_2}}^{\varepsilon_{i_2}+\Delta_\varepsilon} d\varepsilon\, \psi(t \mid \varepsilon)\, \rho(\varepsilon) \right]^{q'} \\ &\approx \frac{1}{(\theta/\Delta_t\,\Delta_\varepsilon)^{q'-1}} \sum_{i_2=-\infty}^{\infty} [\rho(\varepsilon_{i_2})]^{q'}\, \Delta_\varepsilon \\ &\times \sum_{i_1=0}^{\infty} [\psi(t_{i_1} \mid \varepsilon_{i_2})]^{q'}\, \Delta_t. \end{aligned} \tag{28}$$

Here, $\Delta_\varepsilon\,\Delta_t$ is the surface of the elementary rectangle whose side lengths $\Delta_t (\ll \tau_0)$ and $\Delta_\varepsilon (\ll \sigma)$ are arbitrarily small positive numbers while $t_{i_1} = i_1\,\Delta_t$ and $\varepsilon_{i_2} = i_2\,\Delta_\varepsilon$.

In equation (28) summation over variable i_1 is limited from the bottom and over i_2 is unlimited. This means that the study of the generalized partition function scaling with side lengths is impossible. Nevertheless, the answer to the question how it scales with volume fluctuation is still possible, and this is our main interest in this section.

By comparing expressions (28) and (24), so far we find that

$$p_{\underline{i}} \approx \rho(i_2\Delta_\varepsilon)\, \psi(i_1\Delta_t \mid i_2\Delta_\varepsilon)\, \Delta_\varepsilon\Delta_t, \tag{29}$$

equation (29) relates $p_{\underline{i}}$ to a grid of rectangles of equal size. Note that the last summation over i_1 in expression (28) can be performed explicitly

$$\begin{aligned} \sum_{i_1=0}^{\infty} [\psi(t_{i_1} \mid \varepsilon_{i_2})]^{q'} &= [\tau(\varepsilon_{i_2})]^{-q'} \sum_{i_1=0}^{\infty} \exp(-i_1\, q'\, \Delta_t\, /\tau(\varepsilon_{i_2})) \\ &= \frac{[\tau(\varepsilon_{i_2})]^{-q'}}{1-\exp(-q'\,\Delta_t\,/\tau(\varepsilon_{i_2}))} \approx \frac{[\tau(\varepsilon_{i_2})]^{1-q'}}{q'\,\Delta_t}. \end{aligned} \tag{30}$$

When deriving the last approximate equality in equation (30), we had to use the constraint $q'\,\Delta_t/\tau(\varepsilon_{i_2}) \ll 1$, which can always be obeyed as Δ_t is arbitrarily small and q' is a restricted quantity. By introducing expression (30) into (28) we obtain (changing also the summation over i_2 in the third row of (28) by integration) the generalized partition function in the form

$$\begin{aligned} Z(q') &\approx \left(\frac{\tau_0\,\sigma}{M}\right)^{q'-1} \frac{1}{q'} \int_{-\infty}^{\infty} d\varepsilon\, [\rho(\varepsilon)]^{q'}\, [\tau(\varepsilon)]^{1-q'} \\ &= \left(\frac{\sigma}{M}\right)^{q'-1} \frac{1}{q'} \int_{-\infty}^{\infty} d\varepsilon\, [\rho(\varepsilon)]^{q'}\, \exp(\lambda\,(1-q')\,\varepsilon) \\ &= N_{q'}\, \exp(\lambda\mu\,(1-q'))\, J(q'). \end{aligned} \tag{31}$$

In equation (31) the integral

$$J(q') \stackrel{\text{def.}}{=} \int_{-\infty}^{\infty} dy \exp\left(-\frac{q'}{2} \mid y \mid^{\alpha} + \lambda\,\sigma(1-q')y\right) \tag{32}$$

and factor $N_{q'} = \frac{1}{q'} M^{1-2\,q'}$ were obtained after simple changing of variables, $y \stackrel{\text{def.}}{=} (\varepsilon-\mu)/\sigma$, in the integrals in the first and second rows in equation (31). The (dimensionless) denominator θ in expression (28) assumes the form $\theta = M\Delta_t\,\Delta_\varepsilon/\tau_0\,\sigma$ proportional to $\Delta_t\,\Delta_\varepsilon$ to avoid superfluous rectangle there. Note that the $\left(\frac{\sigma}{M}\right)^{q'-1} \frac{1}{q'}$ coefficient leaves normalization of the generalized partition function in equation (31) unchanged. Here $M \stackrel{\text{def.}}{=} 2^{1+1/\alpha}\Gamma(1+1/\alpha)$. In Section 3.1 below, we discuss the scaling form of the generalized partition function and consider useful Rényi dimensions.

3.1 Multiscaling form of the partition function: Rényi dimensions

Since integral $J(q')$ and hence the partition function $Z(q')$ are already calculated in Appendix A, again by using SPA (cf. Eq. (69)), one readily finds that

$$Z(q') \approx B(q')\, L^{-\tau(q')}, \tag{33}$$

where

$$B(q') = M^{1-q'}\, q'^{(1-2\alpha)/2(\alpha-1)} \exp((bc-\lambda\mu)(q'-1)), \tag{34}$$

while c is the constant, which should be chosen so as to make prefactor $B(q')$ independent of the scale L as expected. Therefore,

$$c = \frac{\lambda\mu}{b} \tag{35}$$

and it should be fixed to make the general scaling exponent $\tau(q')$ also independent on L. This condition is possible to fulfil as it is already fixed by relation (45). Therefore, the exponent takes the form (cf. Eq. (69) in Appendix A)

$$\begin{aligned} \tau(q') &= -c\,(1-q') - |1-q'| \left(\frac{|1-q'|}{q'+q_0'}\right)^{1/(\alpha-1)} \\ &= (q'-1)D(q'), \end{aligned} \tag{36}$$

where q_0' is the ad hoc correction constant, which can be estimated by self-consistency of our procedure (cf. relation (i) below). Here, the (positive) Rényi dimensions

$$D(q') = \frac{\tau(q')}{q'-1} = c + sgn(1-q') \left(\frac{|1-q'|}{q'+q_0'}\right)^{1/(\alpha-1)} \tag{37}$$

obey the following relations:

(i) the $\lim_{q'\to 0} D(q') = c + \frac{1}{q_0'^{1/(\alpha-1)}} \equiv q_0' = \frac{1}{[D(0)-c]^{\alpha-1}} \geq 0$ relation, where $D(0) = f(\eta(q'=0)) > c$ (which comes from the comparison of the second relation in (36) with Eq. (42)), cannot be identified here with capacity or box dimension[13] (defined, e.g., in [49]);
(ii) $\lim_{q'\to\infty} D(q') = c - 1 \geq 0$;
(iii) $\lim_{q'\to 1} D(q') = c > 0$;
(iv) the first derivative $D(q')$ over q';

$$D'(q') = -\frac{1}{\alpha-1}\left(\frac{|\,1-q'\,|}{q'+q_0'}\right)^{(2-\alpha)/(\alpha-1)} \times \frac{1+q_0'}{(q'+q_0')^2} \leq 0, \tag{38}$$

which for $q' = \infty$ is equal to 0, while it vanishes at $q' = 1$ for $\alpha < 2$ otherwise (for $\alpha > 2$) it diverges;
(v) the second derivative $D(q')$ over q'

$$D''(q') = \frac{2}{\alpha-1}\left(\frac{|\,1-q'\,|}{q'+q_0'}\right)^{(2-\alpha)/(\alpha-1)} \frac{1+q_0'}{(q'+q_0')^3} + \frac{2-\alpha}{(\alpha-1)^2}\left(\frac{1+q_0'}{(q'+q_0')^2}\right)^2 \times \left(\frac{|\,1-q'\,|}{q'+q_0'}\right)^{(3-2\alpha)/(\alpha-1)} sgn(1-q'), \tag{39}$$

and again equals 0 for $q' = \infty$ and for $\alpha < 3/2$ it vanishes at $q' = 1$, otherwise (for $\alpha > 3/2$) it diverges.

From equation (36) and relation (ii) we obtain for large q', the expression concerning the general exponent

$$\tau(q') \approx (c-1)\,q' = \eta_{min}\,q'. \tag{40}$$

This expression is an important result for the analysis of the spectrum of singularities, as $\eta_{min} = c - 1$ defines its bottom (cf. Sect. 3.2). Moreover, by introducing equation (40) into equation (33) and comparing it with equations (24) and (25), we find (after some manipulations) for $q' \to \infty$

$$p_{\underline{i}}^{max} \approx \theta\, L^{-\eta_{min}}. \tag{41}$$

In equation (41) $p_{\underline{i}}^{max}$ is the maximal value among all local probabilities $p_{\underline{i}}$. Apparently, the generalized partition function for diverging q' is dominated by the maximal local probability, which constitutes a monofractal. The q' power plays the role of the filter, which selects the largest probability value[14]. The self-consistent hypothesis is that all local probabilities scale with L. Hence, it is reasonably to study the spectrum of local scaling exponents (called also pointwise or local dimensions [49] of different fractals placed here in $(\Delta t, \varepsilon)$ half-plane, see Sect. 3.2 below). Therefore, by increasing q' larger and larger the local dimensions are visible less and less. This result gives a coupling, which is a source of q'-dependence of η shown by the first relation in (44) in Section 3.2.

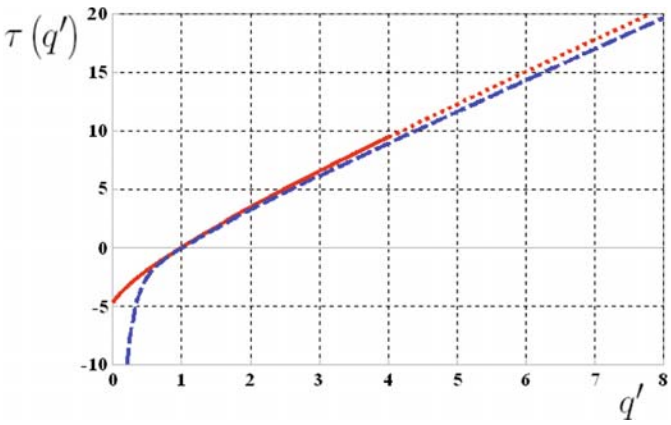

Fig. 3. (Color online) Plot of the general scaling exponent τ vs. order q' at $\alpha = 1.754$ and both for $q_0' = 0$ (lower laying dashed curve) and $q_0' = 1.0$ (upper laying solid and dotted curve), defined only for the positive values of q'. Solid part of the upper curve corresponds to the range of q' values where the MF-CTRW formula satisfactorily fits the empirical data, while the dotted part corresponds to the range where the fit is unsatisfactory (cf. Figs. 1 and 2).

We plotted the general scaling exponent $\tau(q')$ vs. q' for two different examples $q_0' = 0$ (lower laying curve in Fig. 3) and $q_0' = 1$ (upper laying curve in Fig. 3). As it is seen, there is an essential difference between them. That is, this exponent diverges for $q' \to 0$ (according to the power law) in the former case in contrast to the latter case where it is finite. For both examples, for $q' \to \infty$, the general scaling exponent diverges linearly while it vanishes for $q' = 1$. That way, finite Rényi dimensions can be viewed as useful quantities, as they are the most important (multiplicative) parts of the general scaling exponent, describing different interesting properties of the system. For instance, for $q' > 1$ transactions or correlations between them presumably cluster while for $q' = 1$ the Rényi dimension $D(1)$ becomes the Shannon information.

Property (ii) follows directly from equation (37). Hence, as usual [49], our Rényi dimensions are the non-negative, monotonically decreasing functions of q' (cf. Fig. 4). Indistinct (in this scale) kink appears at $q' = 1$. This kink can be considered as a fingerprint of D' singularity and D'' discontinuity at this point (cf. Figs. 5 and 6, respectively).

To make analysis of the Rényi dimensions easier (particularly in the vicinity of $q' = 1$) we plotted in Figure 5 their first derivative, $D'(q')$, given by expression (38), and in Figure 6 its second derivative, $D''(q')$, given by expression (39) (both, e.g., for exponent $\alpha = 1.754$).

Plots shown in Figures 4 and 5 are consistent with that presented in Figure 6. The latter shows that for $3/2 < \alpha < 2$ the limits of second derivative $D''(q' \to 1_-) \to$

[13] Rényi dimension $D(0)$ can be determined here only to some multiplicative factor, cf. Section 3.2.

[14] The analogous role plays q' for its decreasing negative values as it selects the lowest value of the local scaling exponent. However, it is not the case considered here.

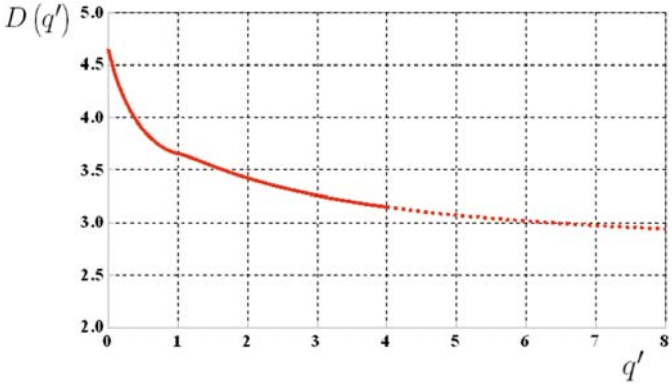

Fig. 4. (Color online) The Rényi dimensions, $D(q')$, vs. order, $q'(\geq 0)$, given by expression (37) for exponent $\alpha = 1.754$ and $q'_0 = 1.0$. The indistinct kink placed at $q' = 1$ suggests a possible singularity of $D'(q')$ at this point (cf. Fig. 5). The second half of $D(q')$ (for $q' < 0$) does not exist within our model.

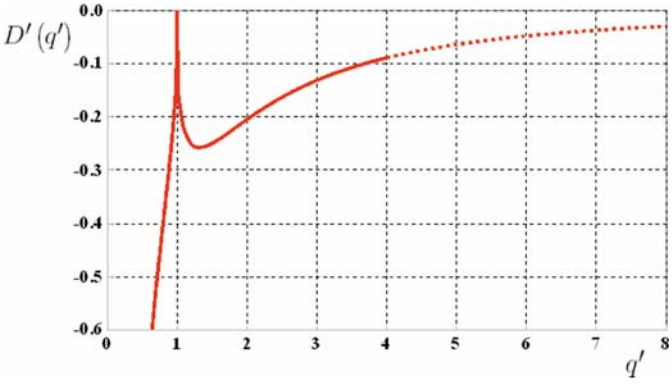

Fig. 5. (Color online) The spike of the first derivative of the Rényi dimensions $D'(q')$ vs. order $q'(\geq 0)$ given by expression (38) for exponent $\alpha = 1.754$ and $q'_0 = 1.0$. The finite height spike of $D'(q')$ is placed at $q' = 1$; its asymmetry is weakly visible.

$-\infty$ and $D''(q' \to 1_+) \to \infty$ mean, that at $q' = 1$ the second derivative, D'', is indefinite, i.e., it has an infinite discontinuity at $q' = 1$. Such a behaviour of the Rényi dimensions and their derivatives is, indeed, responsible for phase transitions considered in Section 4, below.

3.2 Spectrum of local dimensions

Since the scale can be determined up to some arbitrary power ω and hence the general scaling exponent as well as the Rényi dimensions up to some multiplicative factor $1/\omega$, the question arises which definition of scale can be the most appropriate for our analysis. To answer this question, we consider in this section the spectrum of local dimensions in order to construct a self-consistent multifractal procedure.

Since the Legendre (or contact) transformation can be defined here, we obtain the spectrum of local dimensions $f(\eta)$ from the global scaling exponent $\tau(q')$,

$$f(\eta) = q'\,\eta - \tau(q'). \tag{42}$$

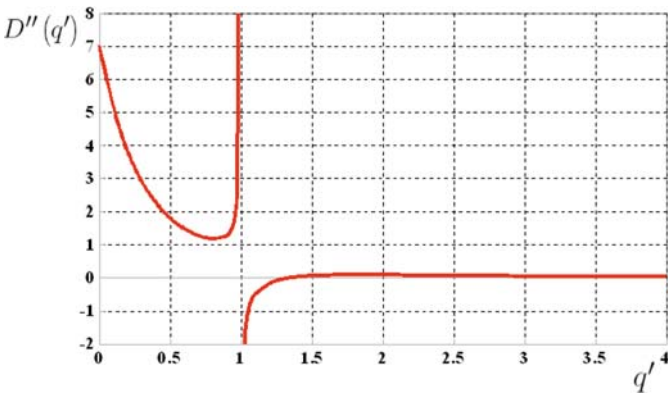

Fig. 6. (Color online) The second derivative of the Rényi dimensions $D''(q')$ vs. order $q'(\geq 0)$ given by expression (39) for exponent $\alpha = 1.754$ and $q'_0 = 1$, obtained from empirical data (cf. Tab. 1). Indeed, q'-dependence of this quantity together with $D'(q')$ one clearly show the existence of singularity at $q' = 1$.

Here, variables

$$\eta(q') = \frac{d\tau(q')}{dq'},$$
$$q' = \frac{d\,f(\eta)}{d\eta}. \tag{43}$$

By combining equations (36)–(38) and (42) we derive an explicit dependence of the spectrum of local dimensions f and local dimension η themselves on the independent variable q',

$$\eta(q') = D(q') + (q'-1)D'(q')$$
$$= c + \left(\frac{|\,1-q'\,|}{q'+q'_0}\right)^{\nu}\left(1+\nu\,\frac{1+q'_0}{q'+q'_0}\right) sgn(1-q'),$$

$$f(\eta(q')) = D(q') + q'(q'-1)D'(q')$$
$$= c + \left(\frac{|\,1-q'\,|}{q'+q'_0}\right)^{\nu}\left(1+\nu\,q'\,\frac{1+q'_0}{q'+q'_0}\right) sgn(1-q'), \tag{44}$$

where $\nu \stackrel{\text{def.}}{=} 1/(\alpha-1)$.

To make equation (42) consistent with equation (40), we assume that $f(\eta = \eta_{min})$ disappears. This assumption supplies an additional condition. From this condition and from the second relation in equation (44) we obtain

$$c = \frac{\alpha + q'_0}{\alpha - 1}, \tag{45}$$

which is complementary to (35). The first relation in (44) does not introduce, for $\eta = \eta_{min}$, a subsequent relation. Obviously, both (35) and (45) conditions reduce the number of free parameters in our model.

Although we obtained an explicit dependence of f on q' (the second relation in (44)), the analogous dependence of

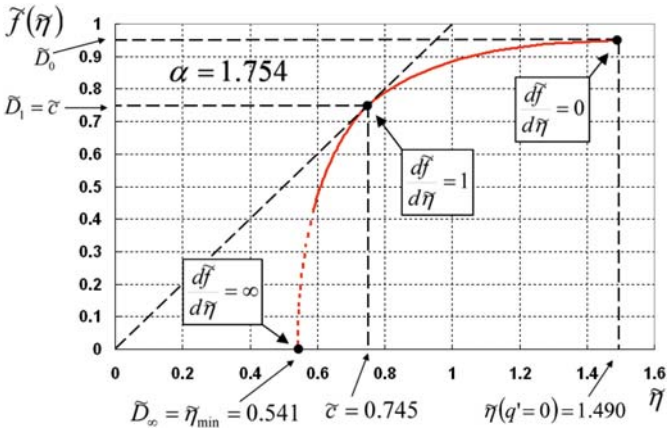

Fig. 7. (Color online) The spectrum of local dimensions $\tilde{f}$ vs. local dimension $\tilde{\eta}$ for exponent $\alpha = 1.754$ (i.e., this spectrum describes the trading on futures at the USDM exchange rate) and $q'_0 = 1.0$. This plot corresponds only to the positive range of q'. Hence, it is truncated at $\tilde{\eta}(q' = 0) = 1.490$. This spectrum, considered within the MF-CTRW model, is valid (roughly speaking) for the range of $(\tilde{\eta}, \tilde{f})$ between point (0.586, 0.421) (obtained from Eqs. (44) for $q' = 4$) and point (1.490, 0.949) (obtained for $q' = 0$), being still sufficiently broad (e.g., it is broader than the $\tilde{\eta}_{min}$ value).

f on η requires, in general, the solution of the entangled, transcendental equation. This equation is derived below by combining both relations given in equation (44),

$$|\eta - c| = \omega_0 \left(1 + q'_0\right) \frac{\left(1 - \frac{f-c}{\eta-c}\right)^{\nu}}{\left(q'_0 + \frac{f-c}{\eta-c}\right)^{\nu+1}}, \; \eta \neq c, \qquad (46)$$

where $sgn(f-c) = sgn(\eta-c) = sgn(1-q')$ and ω_0 was already defined in Section 2.1.2, above. Equation (46) gives solution η (by using the method of successive iterations) as a convex function of f. That is, we have $f \leq \eta$ while equality $\eta = f$ is valid only for a single point $q' = 1$. Additionally, $\eta = c$ for this point. Notably, of a concrete value of the correction constant q'_0 has to be known in order to solve equation (46). For the pathological case of vanishing of the correction constant, this equation reduces to its simplified form

$$\eta = f + \omega_0^{-(\alpha-1)} |f - c|^{\alpha}. \qquad (47)$$

In fact, in Figure 7 the plot of $\tilde{f}$ vs. $\tilde{\eta}$ is shown, where any quantity $\tilde{h} \stackrel{\text{def.}}{=} \omega_0^{-1} h$. In this representation equation (46) takes the simpler form (which is consistent with (42) and both relations in (43)), where ω_0 is absent (and η, c and f are simply replaced by $\tilde{\eta}$, $\tilde{c}$ and $\tilde{f}$, respectively); in this representation both q' and q'_0 remains unchanged. Hence, for example, equation (47) takes simpler form:

$$\tilde{\eta} = \tilde{f} + \mid \tilde{f} - \tilde{c} \mid^{\alpha} . \qquad (48)$$

The width of the spectrum of singularities corresponds to the range $-1 < q < 3$ (shown in Figs. 1 and 2), where prediction of the MF-CTRW model satisfactorily fits the empirical curve $\ln\left(\langle \Delta t^q \rangle / \Gamma(1+q)\right)$. Fortunately, this is the range most important for study of the multifractality (as there the nonlinear q-dependence is placed). Hence, only within the range $\tilde{\eta}(q' = 4) < \tilde{\eta} < \tilde{\eta}(q' = 0)$ the MF-CTRW model can be used to describe empirical data. This restriction still leaves the width of the spectrum sufficiently large. This is the argument for utility of the model to study multifractal properties of intertransation times generated by fluctuations. Another argument, the most important for our work, is that the MF-CTRW model is valid both for $q' = 1$ and its vicinity (cf. plot in Fig. 7 as the derivative $d\tilde{f}/d\tilde{\eta} = 1$ at this point), where indeed phase transitions are investigated. However, the spectrum of singularities is unsensitive to these transitions therefore it is necessary to study phase transitions from the thermodynamic point of view.

Note that some so-called left-sided multifractals (whose spectra of singularities have only the bottom i.e., $f(\eta)$ is shaped like the left half of $\bigcap$) were already investigated in [63] from the mathematical point of view, where authors considered even spectra of singularities having their tops at $\eta = \infty$.

4 Financial higher-order phase transitions

In the present section we prove that intensive trading of the futures on Forex (for example, the archival data at the USDM exchange rate) can exhibit the third-order phase transition for $q' \to 1$ (or $q \to 0$). This phase transition is controlled by the multifractal component of free energy (cf. Tab. 3 and Eq. (36)). We discuss it herein for the range of $\alpha > 3/2$, since

(i) α belonging to this range was, indeed, derived from most of our empirical data (cf. Tab. III in [1]) by using the MF-CTRW formalism;
(ii) for this range of α (except $\alpha = 2$) the lowest (simplest), third-order phase transition was predicted (cf. Eqs. (51) and (52) derived in Sect. 4.1, below).

For exponent $\alpha \leq 3/2$ we predicted even higher-order phase transitions (cf. Tab. 4) but empirical α values from this range (cf. Tab. III in [1]) are burdened by too large statistical errors to make any definite conclusion.

4.1 Remarks on the specific heat

Our considerations are based on the correspondence (shown in Tab. 3) between thermodynamic quantities on the one hand and multifractal ones on the other.

By using this correspondence we exploited the analog of specific heat, which characterizes fluctuations within

Table 3. Correspondence between selected thermodynamic and multifractal quantities.

Thermodynamics	Multifractality
β	q'
V	$b(=\ln(L))$
$E(\beta)/V$	$\eta(q')$
$\beta F(\beta)/V$	$\tau(q')$
$S(E)/V$	$f(\eta)$
$c_V(\beta)$	$c_b(q')$

the multi- and monofractal domains

$$\begin{aligned} c_V(\beta) &= \left(\frac{\partial(E/V)}{\partial T}\right)_V = -T\left(\frac{\partial^2(F/V)}{\partial T^2}\right)_V \\ &= -\beta^2\left(\frac{\partial(E/V)}{\partial \beta}\right)_V = -\beta^2\left(\frac{\partial^2(\beta F/V)}{\partial \beta^2}\right)_V \\ &\equiv -q'^2\left(\frac{\partial^2\tau(q';b)}{\partial q'^2}\right)_b = \left(\frac{\partial\eta(q';b)}{\partial(1/q')}\right)_b = c_b(q'). \end{aligned} \tag{49}$$

Only here (and in the second relation in (50)) we introduced an explicit dependence of some multifractal quantities on b (and therefore used partial derivatives) to emphasize their relations to corresponding thermodynamic quantities. In this derivation we used the following expressions and the correspondence between thermodynamic and multifractal quantities

$$E/V = \left(\frac{\partial(\beta F/V)}{\partial \beta}\right)_V \equiv \eta = \left(\frac{\partial \tau}{\partial q'}\right)_b. \tag{50}$$

The first expression in the last row in equation (49) is the basis for derivation of the explicit q'-dependence of the specific heat, $c(q')$[15].

After calculating of the second derivative, $d^2\tau(q')/dq'^2$, (by using the first equality in Eq. (36)) we finally obtain from equation (49) the expression

$$c(q') = \nu(\nu+1)\left(q'\frac{1+q'_0}{q'+q'_0}\right)^2 \frac{|1-q'|^{\nu-1}}{(q'+q'_0)^{\nu}}. \tag{51}$$

Equation (51) diverges according to power-law $1/|1-q'|^{1-\nu}$ at $q'=1$ only for $\nu<1$ or $\alpha>2$. We examine this crucial formula for the 3rd- and higher-order phase transitions.

In Figure 8 the specific heat given by formula (51) is shown for $\alpha=1.754$ and $q'_0=1$. Again, the prediction of the MF-CTRW formalism within the range of q' values where q-moments well fit the empirical data is represented by the solid curve, while the dotted curve shows the region where they do not fit (cf. Fig. 1).

Although for $q'\to 0$ the specific heat shows singularity (which is a signature of a phase transition), the most interesting and possible for more intensive study is its behaviour in the vicinity of $q'=q'_c=1$. We explain below that in such a case we have to deal with the third-order phase transition. This transition can be roughly interpreted in terms of the transition between the phase (with $q<0\equiv q'<1$) where high frequency trading dominates the q-moment $\langle \Delta t^q\rangle$ and the phase (with $q>0\equiv q'>1$), where the low frequency trading dominates this moment.

[15] The notation of the specific heat $c(q')$ has nothing to do with constant c used earlier e.g., in equations (35) and (45).

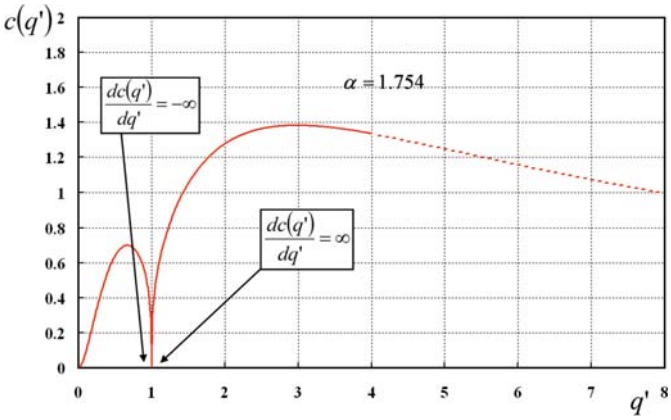

Fig. 8. (Color online) The anti-spike of specific heat $c(q')$ (given by formula (51)) vs. q' (for $\alpha=1.754$ and $q'_0=1$), which exhibits the third-order phase transition at $q'=q'_c=1$ (or at $q=q_c=0$), cf. Figure 9 for completeness.

From equation (51) we obtain,

$$\begin{aligned} \frac{dc(q')}{dq'} &= \frac{2}{q'}c(q') - q'^2\frac{d^3\tau(q')}{dq'^3} \\ &= sgn(1-q')\nu(\nu+1)(1+q'_0)^2 q'\frac{|1-q'|^{\nu-2}}{(q'+q'_0)^{\nu+3}} \\ &\quad\times\{q'\left[q'-\nu-(\nu+1)\,q'_0\right]+2q'_0\}, \end{aligned} \tag{52}$$

which we study for $q'>0$.

In Figure 9 the prediction of formula (52) is presented as a function of q' (again for $\alpha=1.754$ and $q'_0=1$). As it is seen, the first derivative, $\frac{dc(q')}{dq'}$, features an infinitely large discontinuity at $q'=1$. The third-order derivative of the free energy or, more precisely, the third-order derivative of its nonlinear component (cf. expression (36) and Tab. 3) is responsible for this diverging discontinuity. Therefore, we can call this transition the third-order transition.

In Table 4 we summarize recommendations concerning possible phase transitions predicted by our MF-CTRW formalism. Of course, even more detailed analysis can be accomplished by taking higher-order derivatives of $c(q')$ with respect to q'.

5 Summary and concluding remarks

In the present work we used the Multifractal Continuous-Time Random Walk (MF-CTRW) formalism, developed in our recent paper [1], to study statistical and thermodynamic properties of interevent times (intertransaction times or pausing times) recorded when futures at the

Table 4. Orders of possible phase transitions at $q' = 1$ for complementary ranges of α.

Range of α	Range of ν	$c(q'=1)$	$\frac{dc(q')}{dq'}\mid_{q'=1}$	Phase transition
$\alpha \leq 3/2$	$\nu \geq 2$	continuous	continuous	at least 5th order (depends on α)
$3/2 < \alpha < 2$	$1 < \nu < 2$	continuous & diverging	discontinuous & diverging	3rd order
$\alpha = 2$	$\nu = 1$	continuous	continuous	no phase transition
$\alpha > 2$	$\nu < 1$	continuous & diverging	discontinuous & diverging	3rd order

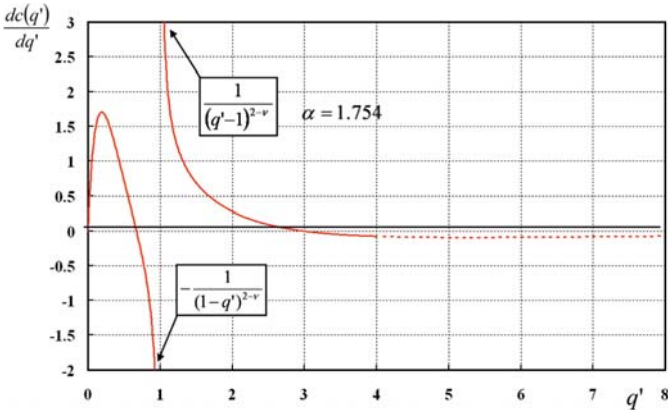

Fig. 9. (Color online) The plot of the first derivative of specific heat, $\frac{dc(q')}{dq'}$, given by formula (52) (for $\alpha = 1.754$ and $q'_0 = 1$) vs. q', whose discontinuity at $q' = q'_c = 1$ (or $q = q_c = 0$) as well as left and right divergences (according to power-laws) are well seen. This plot confirms the third-order phase transition (cf. Fig. 8).

USDM foreign exchange rate on Forex, as a typical example, were intensively traded. That is, we applied the MF-CTRW formalism to describe

(i) The multifractal structure defined (in Sect. 2) by the initial concave and intermediate convex parts of empirical (reduced) q-moments, $\ln\left(\langle \Delta t^q \rangle / \Gamma(1+q)\right)$, of interevent times, presented as a non-linear function of q, cf. plots in Figures 1 and 2 for $-1 < q < 0$ and $0 \leq q < q^1_{ip}(=6.48)$, respectively; for $q \geq q^1_{ip}$ we have again to deal with the concave part. Roughly speaking, apart from the smallest (in the vicinity of $q \approx -1$) and large q values the multifractality occurs.

In this part we found the range $-1 < q < 3$, where prediction of the MF-CTRW model for $\ln\left(\langle \Delta t^q \rangle / \Gamma(1+q)\right)$ satisfactorily fits empirical data. We expect that the model can be applied to descrption of all empirical data forming curves of the shape like those shown in Figures 1 and 2 (cf. also plot in Fig. 2 in Ref. [1]). The multifractality found in Section 2 was, however, insufficient to observe any phase transition.

On the basis of this description we performed two steps. That is,

(ii) we found (by applying the Saddle-Point Approximation) a multifractal scaling equation (33) together with equation (36) of the generalized partition function $Z(q')$ and hence;

(iii) by using the Legendre transformation, we applied the formalism of equilibrium thermodynamics related to global $\tau(q')$ and local $\eta(q')$ exponents to our multifractal system; we considered phase transitions[16] mainly as those of the third order. The formula (51) for the explicit dependence of the specific heat vs. q' was here the key one.

We obtained our results in the form presented, because we used the interevent time distribution in the form of superstatistics, where

(1) the integral kernel, $\rho(\varepsilon)$, was given by the stretched exponential (often used for disordered systems) rather than the exponential function used in the original version of the Continuous-Time Random Walk formalism;
(2) the conditional Pausing-Time Distribution, $\psi(\Delta t \mid \varepsilon)$, was assumed in the Poisson (exponential) form as well as;
(3) the first moment $\langle \Delta t \mid \varepsilon \rangle = \gamma(\varepsilon)$ was assumed that exponentially depends on parameter ε.

Additionally, we extended the comparison of prediction of the heuristic multifractal formula (proposed in our recent paper [1]) with empirical data to the negative q, namely

(iv) we fitted the q-moments $\langle \Delta t^q \rangle / \Gamma(1+q)$, given by the HMF formula within the range $-1 < q \leq 20$, quite well.

Our approach can be considered as complementary to the commonly used Multifractal Detrended Fluctuation Analysis (MF-DFA) [7–9]. Although we are able to transform the scaling exponent $\tau(q')$ into the form required by the MF-DFA method, finding the relation between our approach and the MF-DFA one remains as a challenge (since it is an open question how our qth order partition function relates to the fluctuation function of the corresponding order used in the MF-DFA method).

Concluding, as the most important result concerning the multifractality we considered the third- and higher order phase transitions found at $q = 0$, whose order directly depends on exponent α. These phase transitions can be roughly interpreted as transitions between the phase (with $q < 0$) where high frequency tradings (or short intertransaction times) are most visible and the phase (with $q > 0$) defined by the low frequency tradings (or long intertransaction times). In other words, according to decreasing parameter q, for $q < 0$, better and better visible are shorter and shorter intertransaction times; the reverse situation occurs for increasing q, for $q > 0$.

[16] The system is said to exhibit a phase transition if by a very small continuous change of an appropriate thermal variable the behaviour of the system changes abruptly.

Another interpretation arises from the observation that these phase transitions are driven by the way determining how the probability that q' transactions occur at any rectangle $(\Delta_t, \Delta_\varepsilon)$ (cf. Sect. 3) passes the situation when $q' = 1$. That is, transition between the situation where more than single transation occurs ($q' > 1$) to the situation, where less than one ($q' < 1$) occurs can here be interpreted as the higher-order phase transition.

The higher-order phase transitions is uncommon in the real world and (to our knowledge) was found herein for the first time on the financial market. The order of the phase transition can classify the global measure of the risk. When this order is higher, then finding discontinuity is more difficult (as it is more hidden) and, hence, investor activity can be less risky and more intense. Therefore, if an investor would like to trade less risky assets he or she should avoid such time series, which supply the lowest (the first and/or the second) order phase transitions and left those, which exhibit the higher-order phase transitions between localized ($q' > 1$) and delocalized ($q' < 1$) phases.

We hope that this finding will inspire investors to consider not only the dynamics of financial instrument itself but at least (i) its first derivative (or velocity); (ii) its acceleration (or the second derivative of the instrument) as well as (iii) its jerk (or the third derivative). Hence, for example, the higher order volatilities and correlations should be also considered (cf. [67]).

Two of us (A.K. and R.K.) wish to thank the Organizers of the *7th International Conference "Applications of Physics in Financial Analysis" & Tokyo Tech – Hitotsubashi Interdisciplinary Conference "New Approaches to the Analysis of Large-Scale Business and Economic Data"* for their financial support. Two of us (A.K. and R.K.) thank Didier Sornette and Armin Bunde for useful discussions. Two of us (J.P. and J.M.) wish to thank the Ministerio of Ciencia e Innovación for partial financial support under contract FIS 2009-09689.

Appendix A: Calculation of the integral J(q′)

In the present section we calculate, by using the Saddle-Point Approximation, the basic integral

$$J(q') = \int_{-\infty}^{\infty} dy \exp\left(-\frac{q'}{2} \mid y \mid^{\alpha} + \lambda\sigma(1-q')y\right) \quad (53)$$

and, hence, the generalized partition function

$$Z(q') \approx N_{q'} \exp(\lambda(1-q')\mu)\, J(q'), \quad (54)$$

where the factor $N_{q'}$ is

$$N_{q'} = \frac{1}{q'} M^{1-2q'}. \quad (55)$$

and the coefficient M is defined as

$$M = 2^{1+1/\alpha}\Gamma(1+1/\alpha). \quad (56)$$

In order to evaluate the integral (53), first, we change the integration variable $y = \kappa x$, (where $\kappa > 0$), which results in

$$J(q') = \kappa \int_{-\infty}^{\infty} \exp\left[-f(x)\right] dx \quad (57)$$

where

$$f(x) = \frac{q'}{2} \mid \kappa x \mid^{\alpha} - sgn(1-q')\kappa\lambda\sigma \mid 1-q' \mid x. \quad (58)$$

By assuming that coefficients at both powers of variable x are equal, we obtain

$$\kappa = \left[2\frac{\lambda\sigma \mid 1-q' \mid}{q'}\right]^{1/(\alpha-1)}. \quad (59)$$

Hence, integral $J(q')$ takes the form

$$J(q') = \kappa \int_{-\infty}^{\infty} \exp\left[-\frac{q'\kappa^{\alpha}}{2} h(x)\right] dx, \quad (60)$$

where

$$h(x) = \mid x \mid^{\alpha} - sgn(1-q')x. \quad (61)$$

Now, we are ready to go for both steps of SPA for the calculation of integral $J(q')$:

(i) approximation of the function $h(x)$ by the parabolic expansion around its minimum x_0,

$$h(x) \approx h(x_0) + \frac{1}{2}h''(x_0)(x-x_0)^2, \quad (62)$$

where minimum

$$x_0 = \frac{sgn(1-q')}{\alpha^{1/(\alpha-1)}} \quad (63)$$

while

$$\begin{aligned} h(x_0) &= \frac{1}{\alpha^{\alpha/(\alpha-1)}} - \frac{1}{\alpha^{1/(\alpha-1)}} \\ &= -\frac{\alpha-1}{\alpha^{\alpha/(\alpha-1)}} < 0, \\ h''(x_0) &= \alpha(\alpha-1) \mid x_0 \mid^{\alpha-2} \\ &= (\alpha-1)\,\alpha^{1/(\alpha-1)} > 0, \end{aligned} \quad (64)$$

and, next;

(ii) the explicit calculation of the Gaussian integral (based on the quadratic part of $h(x)$ function) as an approximation of $J(q')$, namely

$$\begin{aligned} J(q') &\approx \kappa \exp\left[-\frac{q'\kappa^{\alpha}}{2} h(x_0)\right] \\ &\quad \times \int_{-\infty}^{\infty} \exp\left[-\frac{q'\kappa^{\alpha}}{4} h''(x)(x-x_0)^2\right] dx \\ &= \frac{2\kappa\sqrt{\pi}}{\sqrt{q'\kappa^{\alpha}h''(x_0)}} \exp\left[-\frac{q'\kappa^{\alpha}}{2} h(x_0)\right]. \end{aligned} \quad (65)$$

Finally, by introducing expressions (64) into (65) and using definition of κ (59) we obtain

$$J(q') = \left(\frac{2\pi}{\alpha-1}\right)^{1/2} \left[\frac{2}{\alpha}(\lambda\sigma)^{2-\alpha}\right]^{1/2(\alpha-1)} \times \left(\frac{\mid 1-q' \mid^{2-\alpha}}{q'}\right)^{1/2(\alpha-1)} \times \exp\left[b\left(\frac{\mid 1-q' \mid^{\alpha}}{q'}\right)^{1/(\alpha-1)}\right], \quad (66)$$

where

$$b = \omega_0^{-1}\,(2^{1/\alpha}\lambda\sigma)^{\alpha/(\alpha-1)}, \quad (67)$$

here $\omega_0 \stackrel{\text{def.}}{=} \alpha^{\alpha/(\alpha-1)}/(\alpha-1)$.

By using the last row in expression (31) we obtain the formula for the generalized partition function

$$Z(q') \approx N_{q'}\left(\frac{2\pi}{\alpha-1}\right)^{1/2} \left[\frac{2}{\alpha}(\lambda\sigma)^{2-\alpha}\right]^{1/2(\alpha-1)} \times \left(\frac{\mid 1-q' \mid^{2-\alpha}}{q'}\right)^{1/2(\alpha-1)} \times \exp\left[\lambda\mu(1-q') + b\left(\frac{\mid 1-q' \mid^{\alpha}}{q'}\right)^{1/(\alpha-1)}\right]. \quad (68)$$

In order to return to normalized $Z(q')$ (i.e. to the partition function obeying (26)), we have to neglect a part of the prefactor of equation (68). Thus, our final rough approximation for the partition function is

$$Z(q') \approx M^{1-q'}\, q'^{(1-2\alpha)/2(\alpha-1)} \times \exp\left[\lambda\mu(1-q') + b\left(\frac{\mid 1-q' \mid^{\alpha}}{q'+q'_0}\right)^{1/(\alpha-1)}\right], \quad (69)$$

where the correction constant q'_0 should be estimated from the requirement of self-consistency of the approach while its exact value should be obtained by comparing the prediction of the approach with the corresponding empirical data. This $Z(q')$ is further considered in Section 3. Beside the normalization obeyed by expression (69), $Z(q')$ takes (for $\alpha = 2$) the form defined by the Gaussian kernel $\rho(\varepsilon)$, which can be derived by independent, exact calculations, without applying SPA.

References

1. J. Parelló, J. Masolivar, A. Kasprzak, R. Kutner, Phys. Rev. E **78**, 036108 (2008)
2. W.A. Fuller, *Introduction to Statistical Time Series* (J. Wiley, Ames Iowa, 1976)
3. M.B. Pristley, *Non-linear and Non-Stationary Time Series Analysis* (Acad. Press, London, 1988)
4. B. Torrésani, *Special Issue on Wavelet and Time-Frequency Analysis*, J. Math. Phys. 39 (1998)
5. J.C. Sprott, *Chaos and Time-Series Analysis* (Acad. Press, London, 2003)
6. *Handbook of Time Series Analysis: Recent Theoretical Developments and Applications*, edited by B. Schelter, M. Winterhalder, J. Timmer (Wiley-VCH, Weinheim, 2006)
7. C.-K. Peng, S.V. Buldyrev, S. Havlin, M. Simons, H.E. Stanley, A.L. Goldberger, Phys. Rev. E **49**, (1994) 1685
8. J.W. Kantelhardt, E. Koscielny-Bunde, H.H.A Rego, S. Havlin, A. Bunde, Physica A **295**, 441 (2001)
9. J.W. Kantelhardt, S.A. Zschiegner, E. Koscielny-Bunde, S. Havlin, A. Bunde, H.E. Stanley, Physica A **316**, 82 (2002)
10. A. Carbone, G. Castelli, H.E. Stanley, Phys. Rev. E **69**, 026105 (2004)
11. E. Alessio, A. Carbone, G. Cstelli, V. Frappietro, Eur. Phys. J. B **27**, 197 (2002)
12. D. Grech, Z. Mazur, Acta Phys. Pol. B **36**, 2403 (2005)
13. A.R. Bishop, G. Grüna, B. Nicolaenko, Physica D **23**, 1 (1987)
14. A. Aharony, J. Feder, Physica D **38**, 1 (1989)
15. F. Schmitt, D. Schertzer, S. Lovejoy, Appl. Stochastic Models Data Anal. **15**, 29 (1999)
16. O. Pont, J.M.D. Delgado, A. Turiel, C.J. Pérez-Vincente, New J. Phys. (2008), in print
17. J.F. Muzy, J. Delour, E. Bacry, Eur. Phys. J. B **17**, 537 (2000)
18. R.N. Mantegna, Physica A **179**, 232 (1991)
19. D. Sornette, *Critical Phenomena in Natural Sciences. Chaos, Fractals, Selforganization and Disorder: Concepts and Tools* (Springer-Verlag, Berlin, 2000)
20. F. Mainardi, M. Raberto, R. Gorenflo, E. Scalas, Physica A **287**, 468 (2000)
21. E.W. Montroll, G.H. Weiss, J. Math. Phys. **6**, 167 (1965)
22. H. Scher, M. Lax, Phys. Rev. B **7**, 4491 (1973)
23. H. Scher, E.W. Montroll, Phys. Rev. B **12**, 2455 (1975)
24. G. Pfister, H. Scher, Phys. Rev. B **15**, 2062 (1977)
25. G. Pfister, H. Scher, Adv. Phys. **27**, 747 (1978)
26. E.M. Montroll, B.J. West, in *Fluctuation Phenomena*, SSM, Vol. VII, edited by E.W. Montroll, J.L. Lebowitz (North-Holland, Amsterdam, 1979), p. 61
27. E.M. Montroll, M.F. Shlesinger, in *Nonequilibrium Phenomena II, From Stochastics to Hydrodynamics*, SSM, Vol. XI, edited by J.L. Lebowitz, E.M. Montroll (North-Holland, Amsterdam, 1984), p. 1
28. G.W. Weiss, *A Primer of Random Walkology*, in *Fractals in Science*, edited by A. Bunde, S. Havlin, (Springer-Verlag, Berlin, 1995), Chap. 5, p. 119
29. E.J. Moore, J. Phys. C: Proc. Phys. Soc. London **7**, 339 (1974)
30. E. Scalas, R. Gorenflo, F. Mainardi, Phys. Rev. E **69**, 011107 (2004)
31. J. Masoliver, M. Montero, J. Parelló, G.H. Weiss, J. Economic Behavior Org. **61**, (2006) 577
32. R. Kutner, Chem. Phys. **284**, 481 (2002)
33. R. Kutner, F. Switała, Eur. Phys. J. B **33**, 495 (2003)
34. R. Kutner, F. Switała, Quant. Finance **3**, 201 (2003)
35. K.W. Kehr, R. Kutner, K. Binder, Phys. Rev. B **23**, 4931 (1981)
36. J.W. Haus, K.W. Kehr, Phys. Rep. **150**, 263 (1987)
37. G. Zumofen, J. Klafter, A. Blumen, *Models for Anomalous Diffusion*, in *Disorder Effects on Relaxational processes. Glasses, Polymers, Proteins*, edited by R. Richert, A. Blumen (Springer, Berlin, 1994), Chap. 8, p. 251

38. T. Wichmann, K.W. Kehr, J. Phys.: Condens. Matter **7**, (1995) 717
39. J. Klafter, G. Zumofen, M.F. Shlesinger, in *Lévy Flights and Related Topics in Physics*, LNP, 450, edited by M.F. Shlesinger, G.H. Zaslavsky, U. Frisch (Springer, Berlin, 1995), p. 196
40. C. Monthus, J.-P. Bouchaud, J. Phys. A: Math. Gen. **29**, 3847 (1996)
41. G. Zumofen, J. Klafter, M.F. Shlesinger, *Lévy Flights and Lévy Walks Revisited*, in *Anomalous Diffusion. From Basics to Applications*, LNP, 519, edited by R. Kutner, A. Pękalski, K. Sznajd-Weron (Springer, Berlin, 1999) p. 15
42. R. Kutner, M. Regulski, Physica A **264**, 107 (1999)
43. R. Hilfer, *Fractional Time Evolution*, in *Applications of Fractional Calculus in Physics*, edited by R. Hilfer (World Scient., Singapore, 2000), p. 87
44. D. ben-Avraham, S. Havlin, *Diffusion and Reactions in Fractals and Disordered Systems* (Cambridge Univ. Press, Cambridge, 2000)
45. M. Kozłowska, R. Kutner, Physica A **357**, 282 (2005)
46. B. Mandelbrot, R.L. Hudson, *The (Mis)Behavior of Markets. A Fractal View of Risk, Ruin, and Reward* (Basic Books, New York, 2004)
47. L. Li, Y. Meurice, Phys. Rev. D **73**, 036006-1 (2006)
48. Th.H. Halsey, M.H. Jensen, L.P. Kadanoff. I. Procaccia, B.I. Shraiman, Phys. Rev. A **33**, 1141 (1986)
49. C. Beck, F. Schlögl, *Thermodynamics of chaotic systems. An introduction* (Cambridge Univ. Press, Cambridge, 1995)
50. L. Harris, J. Financ. Quant. Anal. **22**, 127 (1987)
51. W.M. Fong, W.F. Lab-sane, Quant. Finance **3**, 184 (2003)
52. B. Castaing, Y. Gagne, E. Hopfinger, Physica D **46**, 177 (1990)
53. B. Chabaud, A. Naert, J. Peinke, F. Chillà, B. Castaing, B. Hebral, Phys. Rev. Lett. **73**, 3227 (1994)
54. C. Tsallis, Braz. J. Phys. **39**, 337 (2009)
55. C. Beck, E.G.D. Cohen, Physica A **322**, 267 (2003)
56. C. Beck, E.G.D. Cohen, S. Rizzo, Europhysics News **36/6**, 189 (2005)
57. J.-P. Bouchaud, A. Georges, Phys. Rep. **195**, 127 (1990)
58. J.P. Bouchaud, in *Lévy Flights and Related Topics in Physics*, LNP, 450, edited by M.F. Shlesinger, G.H. Zaslavsky, U. Frisch (Springer, Berlin, 1995), p. 239
59. R. Metzler, J. Klafter, Phys. Rep. **339**, 1 (2000)
60. R.N. Mantegna, H.E. Stanley, *An Introduction to Econophysics, Correlations and Complexity in Finance* (Cambridge Univ. Press, Cambridge, UK, 2000)
61. W. Paul, J. Baschnagel, *Stochastic Processes, From Physics to Finance* (Springer, Berlin 1999)
62. Th. Niemeijer, J.M.J. van Leeuwen, in *Phase Transitions and Critical Phenomena*, edited by C. Domb, M.S. Green (Acad. Press, London, 1976), Vol. 6
63. B.B. Mandelbrot, C.J.G. Evertsz, in *Fractals and Disordered Systems*, 2nd revised and enlarged edn., edited by A. Bunde, Sh. Havlin (Springer, Berlin, 1996)
64. H.E. Stanley, *Fractals and Multifractals: The Interplay of Physics and Geometry* in *Fractals and Disordered Systems*, Second Revised and Enlarged Edition, edited by A. Bunde, Sh. Havlin (Springer, Berlin 1996).
65. R. Badii, A. Politi, *Complexity. Hierarchical structures and scaling in physics* (Cambridge Univ. Press, Cambridge 1997)
66. W.G. Hanan, J. Gough, D.M. Heffernan, Phys. Rev. E **63**, 011109 (2000)
67. N.F. Johnson, P. Jefferies, P.M. Hui, *Financial Market Complexity* (Oxford Univ. Press, Oxford, 2003)